JACS
JOURNAL OF THE AMERICAN CHEMICAL SOCIETY
Communication
pubs.acs.org/JACS

Metal–Organic Frameworks with Precisely Designed Interior for Carbon Dioxide Capture in the Presence of Water

Alejandro M. Fracaroli,[†] Hiroyasu Furukawa,[†] Mitsuharu Suzuki,[†] Matthew Dodd,[§] Satoshi Okajima,[†] Felipe Gándara,[†] Jeffrey A. Reimer,[§] and Omar M. Yaghi*[,†,‡]

[†]Department of Chemistry, University of California—Berkeley, Materials Sciences Division, Lawrence Berkeley National Laboratory, and Kavli Energy NanoSciences Institute at Berkeley, Berkeley, California 94720, United States

[‡]King Fahd University of Petroleum and Minerals, Dhahran 34464, Saudi Arabia

[§]Department of Chemical and Biomolecular Engineering, University of California—Berkeley, and Environmental Energy Technologies Division, Lawrence Berkeley National Laboratory, Berkeley, California 94720, United States

Supporting Information

ABSTRACT: The selective capture of carbon dioxide in the presence of water is an outstanding challenge. Here, we show that the interior of IRMOF-74-III can be covalently functionalized with primary amine (IRMOF-74-III-CH_2NH_2) and used for the selective capture of CO_2 in 65% relative humidity. This study encompasses the synthesis, structural characterization, gas adsorption, and CO_2 capture properties of variously functionalized IRMOF-74-III compounds (IRMOF-74-III-CH_3, -NH_2, -CH_2NHBoc, -$CH_2NMeBoc$, -CH_2NH_2, and -CH_2NHMe). Cross-polarization magic angle spinning ^{13}C NMR spectra showed that CO_2 binds chemically to IRMOF-74-III-CH_2NH_2 and -CH_2NHMe to make carbamic species. Carbon dioxide isotherms and breakthrough experiments show that IRMOF-74-III-CH_2NH_2 is especially efficient at taking up CO_2 (3.2 mmol of CO_2 per gram at 800 Torr) and, more significantly, removing CO_2 from wet nitrogen gas streams with breakthrough time of 610 ± 10 s g^{-1} and full preservation of the IRMOF structure.

Carbon dioxide capture from combustion sources such as flue gas in power plants is an outstanding challenge because CO_2 has to be selectively removed from other gases and, most importantly, water.[1] Porous materials can trap CO_2 in voluminous amounts, but when water is present the efficiency of capture is significantly reduced, as water competes for the binding sites within the pores.[2] Aqueous monoethanolamine (MEA) solutions are efficient at binding CO_2; however, they present a major energy cost and environmental hazard.[3] Thus, a need exists to develop materials capable of addressing this carbon capture challenge.

The preferred method for measuring the efficiency of a given material for capture of CO_2 is to expose a solid form of the material to a mixture of gases containing CO_2 and water, and then to detect the gases and measure the time they take to pass through the material (breakthrough time).[4] Various porous materials[5] such as zeolites, mesoporous silica, polymeric resins, porous carbon, and metal–organic frameworks (MOFs) are being studied for their CO_2 capture properties, but a viable class of materials for this application has yet to emerge. Although carbon capture in mesoporous materials and carbon has been shown under humid conditions,[4c] MOFs show special promise because of their adjustable chemical functionality, structural diversity, and ease of functionalization.[6] Capture of CO_2 from dry gas mixtures (nitrogen, methane, and oxygen) has been reported in MOFs incorporating amines bound to either metal sites[7] or organic linkers.[8] However, successful demonstrations of MOFs capable of CO_2 capture in the presence of water, and doing so without degradation of performance as a result of competition with water, remain uncommon.[4b]

In this Communication, we show how the interior of porous MOFs can be designed to overcome the complications presented by the competition of water with CO_2. We chose a MOF constructed from magnesium oxide rods joined by terphenylene organic linkers {IRMOF-74-III, Mg_2(DH3PhDC), where H_4DH3PhDC = 2′,5′-dimethyl-3,3″-dihydroxy-[1,1′:4′,1″-terphenyl]-4,4″-dicarboxylic acid, Figure 1} to make an extended structure with an **etb** topology supporting one-dimensional channels of 25 Å in their diagonal.[9] The organic linkers and their corresponding IRMOF-74-III structures were functionalized with -CH_3, -NH_2, -CH_2NHBoc, -$CH_2NMeBoc$, -CH_2NH_2, and -CH_2NHMe (Boc = *tert*-butyloxycarbonyl), which point toward the center of the channels (Figure 1). Here, we report the synthesis, characterization, porosity, and CO_2 capture properties (in dry and wet nitrogen streams) of IRMOF-74-III with the six different functionalities, *vide supra*. We find that at low pressure IRMOF-74-III-CH_2NH_2 and -CH_2NHMe exhibit strong binding of CO_2 and have the highest uptake, and that in breakthrough experiments the -CH_2NH_2 form shows selectivity toward CO_2 in a wet nitrogen gas stream with 65% relative humidity (RH). Indeed, the behavior of this material under wet conditions remains unchanged from that observed under dry gas stream.

The synthesis of the appropriate linkers for IRMOF-74-III compounds is shown in Figure 1. Starting from the commercially available methyl 2-hydroxy-4-iodobenzoate (**1**),

Received: April 2, 2014
Published: June 9, 2014

   dx.doi.org/10.1021/ja503296c | *J. Am. Chem. Soc.* 2014, 136, 8863–8866

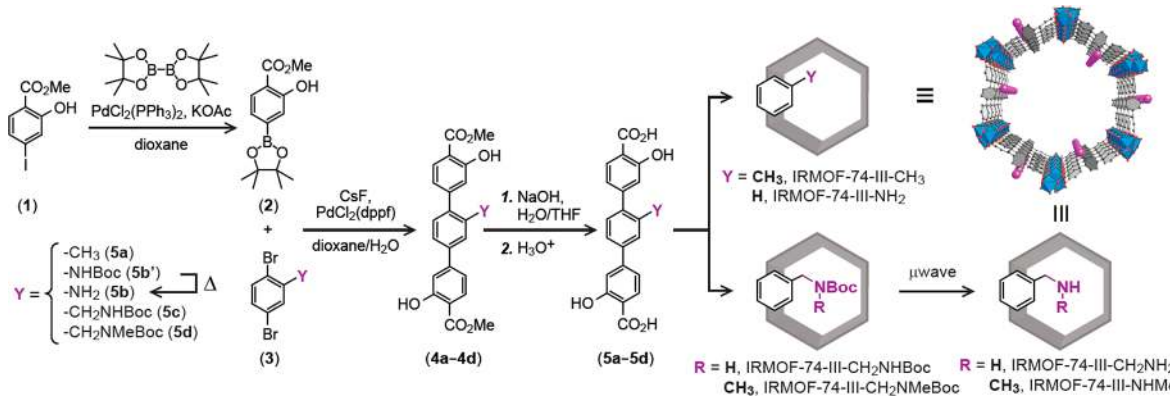

Figure 1. Synthetic pathway for the functionalized organic linkers used in the synthesis of IRMOF-74-III. This methodology allowed us to prepare -CH_3 (**5a**), -NH_2, (**5b**), -CH_2NHBoc (**5c**), and -$CH_2NMeBoc$ (**5d**) functionalized linkers. On the right is shown a schematic representation of the IRMOF-74-III pore as functionalized with the organic linkers **5a**–**5d** and post-synthetic deprotection of Boc groups. Color code: C in gray, O in red, functional groups in purple, Mg as blue polyhedra.

we synthesized four different organic linkers by using Suzuki–Miyaura coupling of boronic acid pinacol ester (**2**) and functionalized 1,4-dibromobenzenes (**3**), followed by saponification reaction of the methyl ester linker derivatives (**4a**–**4d**). The synthetic method was designed to achieve versatility in the covalent incorporation of a variety of functional groups within the pores of IRMOF-74-III. The linkers **5a**–**5d** have -CH_3, -NH_2, -CH_2NHBoc, and -$CH_2NMeBoc$ functional groups, respectively. We have employed the Boc protecting group in order to introduce -CH_2NH_2 and -CH_2NHMe into IRMOF-74-III, as the unprotected amines may react with the metal ions used for the MOF structure synthesis. The synthesized linkers were fully characterized by nuclear magnetic resonance (^1H and ^{13}C NMR) and electrospray ionization mass spectrometry (ESI-MS), and single-crystal X-ray diffraction (XRD) in the case of -NH_2 and -$CH_2NMeBoc$ linkers [section S1, Supporting Information (SI)].

Four IRMOF-74-III structures incorporating **5a**–**5d** were prepared according to reported conditions.[9] The synthesis of IRMOF-74-III-CH_2NHBoc is typical: a solvent mixture containing $Mg(NO_3)_2{\cdot}6H_2O$ (160 mg, 0.62 mmol), linker **5c** (90 mg, 0.19 mmol), and 15 mL of *N*,*N*-dimethylformamide (DMF)/ethanol/water (9:0.5:0.5) was placed in a 20 mL capped vial, which was heated at 120 °C for 20 h. Depending on the functionality incorporated in the interior of the MOF, white (-CH_3), yellow (-NH_2), or pale yellow (-CH_2NHBoc and -$CH_2NMeBoc$) microcrystalline solids were obtained (Figure S3).

The Boc protecting groups in IRMOF-74-III-CH_2NHBoc and -$CH_2NMeBoc$ were removed using a modification of a reported post-synthetic deprotection procedure.[10] In our case, microwave heating was applied (230 °C) for 10 min in a ternary mixture of solvents [2-ethyl-1-hexanol/ethylene glycol/water (9.1:0.5:0.5)]. This process allowed us to quantitatively obtain the unprotected primary (-CH_2NH_2) and secondary amine (-CH_2NHMe) groups in the interior of those MOFs. The successful deprotection was examined by solution ^1H NMR spectra of the digested samples in 50 mM DCl in a DMSO-d_6/D_2O mixture, where the absence of the corresponding Boc group resonance peaks at δ = 1.35 ppm and δ = 1.28 ppm was confirmed for IRMOF-74-III-CH_2NH_2 and -CH_2NHMe, respectively. Similar NMR analysis was carried out for the remaining IRMOF-74-III structures and confirmed the presence of the appropriate functionality (section S4, SI).

To evaluate the porosity and crystallinity of these materials, as-synthesized samples were activated by immersion in 10 mL of DMF for 4 h, the liquid was decanted, and then the process was repeated three times per day for 3 days. This whole protocol was repeated with methanol during 3 additional days to obtain the solid with washed interior. The solvent within the pores of the resulting solids was removed under dynamic vacuum initially at room temperature and then by heating at 120 °C for 12 h. The crystallinity and structure of the evacuated series of IRMOF-74-III compounds were confirmed by the coincidence of the sharp powder X-ray diffraction (PXRD) lines with those of the parent unfunctionalized IRMOF-74-III (section S5, SI). In addition, PXRD analysis of the IRMOF-74-III-CH_2NH_2 and -CH_2NHMe samples further confirmed that the frameworks maintain their structural integrity and porosity after post-synthetic deprotection of the Boc groups. Nitrogen adsorption isotherms were measured at 77 K, and the Brunauer–Emmett–Teller (BET) surface areas were calculated to be 2640, 2720, 2170, 2220, 2310, and 2250 $m^2\ g^{-1}$ for IRMOF-74-III-CH_3, -NH_2, -CH_2NHBoc, -$CH_2NMeBoc$, -CH_2NH_2, and -CH_2NHMe, respectively. These values are similar to the BET surface area of the parent IRMOF-74-III (2440 $m^2\ g^{-1}$),[9] indicating that porosity is maintained in the functionalized as well as the deprotected forms.

The CO_2 uptake capacity for each of the functionalized IRMOF-74-III compounds was obtained by measuring the corresponding isotherms at 25 °C (Figure 2a). All the compounds showed significant CO_2 uptake, and, as expected, IRMOF-74-III-CH_3, -NH_2, -CH_2NH_2, and -CH_2NHMe exhibit similar capacity at 800 Torr, while the protected compounds IRMOF-74-III-CH_2NHBoc and -$CH_2NMeBoc$ showed lesser uptake because of the sterically bulky Boc groups (Figure 2a). Interestingly, IRMOF-74-III-CH_2NH_2 and -CH_2NHMe showed the highest uptake capacities at low CO_2 pressure range (<1 Torr, Figure 2b) with hysteresis, retaining ca. 20 $cm^3\ g^{-1}$ of CO_2 upon desorption down to 10 Torr (Figure 2a). This trend can be attributed to the strong interactions between CO_2 and aliphatic amine functionalities. A second CO_2 isotherm was recorded after evacuation of the sample at room temperature for 2 h (second cycle, Figure 2c). As expected, the initial slope of the CO_2 uptake in the second cycle for IRMOF-74-III-CH_2NH_2 and -CH_2NHMe was 1/3.6 and 1/4.6 compared to the first cycle, and the maximum uptakes at 800 Torr were less than those of the first cycles (by ca. 18 and 15 $cm^3\ g^{-1}$ for

dx.doi.org/10.1021/ja503296c | J. Am. Chem. Soc. 2014, 136, 8863–8866

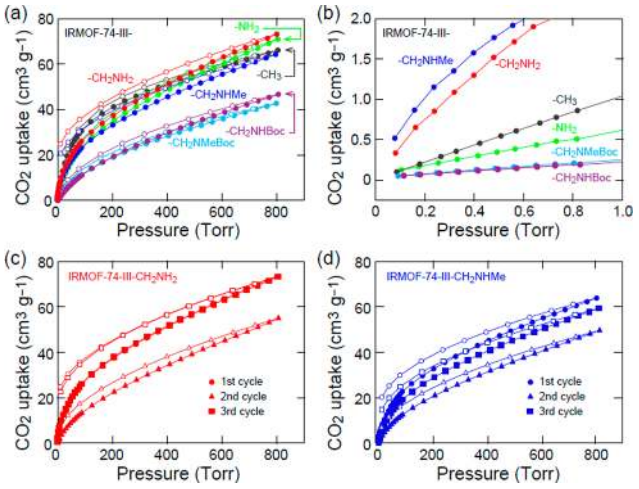

Figure 2. (a) Comparison of CO_2 uptake at 25 °C for IRMOF-74-III-CH_3 (gray), -NH_2 (green), CH_2NH_2 (red), -CH_2NHMe (blue), -CH_2NHBoc (purple), and -CH_2NMeBoc (cyan). (b) Expansion of the low pressure range (>1 Torr). Carbon dioxide isotherms at 25 °C for IRMOF-74-III-CH_2NH_2 (c) and -CH_2NHMe (d). Uptakes for samples after activation (first cycle), after first CO_2 uptake (second cycle), and after 120 °C heating for 1 h for regeneration (third cycle) are shown in circles, triangles, and squares, respectively.

IRMOF-74-III-CH_2NH_2 and -CH_2NHMe, respectively). As this evidence clearly indicated a strongly bound CO_2, the solids were heated to 120 °C under vacuum (10 mTorr) for 1 h, and isotherms for the third cycle of CO_2 uptake were measured. In the case of IRMOF-74-III-CH_2NH_2, the CO_2 was fully desorbed, while partial desorption was observed for IRMOF-74-III-CH_2NHMe (third cycle, Figure 2c,d).

Cross-polarization magic angle spinning ^{13}C NMR spectra were collected for each of IRMOF-74-III-NH_2, -CH_2NHBoc, -CH_2NH_2, and -CH_2NHMe to evaluate the possibility of carbamate formation, which would be expected in the reaction of CO_2 with IRMOF-74-III-CH_2NH_2 and -CH_2NHMe and not the others. Activated samples of these MOFs were exposed to ^{13}C-labeled CO_2 at room temperature and ca. 760 Torr for 24 h before the samples were transferred into a solid-state NMR rotor. The ^{13}C NMR spectra of IRMOF-74-III-CH_2NH_2 and -CH_2NHMe show a broad resonance peak centered at δ = 160 ppm, corresponding to the chemical shift of carbamate species resonance (carbamate ions and carbamic acid) reported in the literature,[4a,11] while in the case of IRMOF-74-III-NH_2 and -CH_2NHBoc samples, this peak is absent (Figure S18). This difference in the ^{13}C NMR spectra confirms that CO_2 is only chemisorbed by -CH_2NH_2 and -CH_2NHMe amine-functionalized IRMOF-74-III, but not by MOFs with -NH_2 and -CH_2NHBoc functionalities.

Given the fully reversible nature of the CO_2 uptake of IRMOF-74-III-CH_2NH_2 (Figure 2c), we carried out a dynamic separation experiment to evaluate the breakthrough time in the absence and presence of water. Here, a solid sample of IRMOF-74-III-CH_2NH_2 compound (238 mg, 0.56 mmol) was packed in a 10 cm length × 0.6 cm diameter stainless steel column and utilized as an adsorbent bed. A mixed gas containing 16% (v/v) of CO_2 in a nitrogen gas stream was introduced to the column, and the effluent was monitored by a mass spectrometer.[4] The breakthrough time was determined when the CO_2 concentration in the effluent reached 5% of the influent concentration.

Under dry conditions, the IRMOF-74-III-CH_2NH_2 adsorbent bed held CO_2 up to 670 ± 10 s g^{-1}, which is equivalent to a kinetic CO_2 adsorption capacity of 0.8 mmol g^{-1}. The CO_2 influent was then stopped and, to regenerate the material, we purged the adsorbent bed with dry nitrogen; however, this was not enough to fully remove adsorbed CO_2 (Figure 3a). Therefore, the sample bed was heated at 95 °C under nitrogen flow for 30 min, upon which appearance of CO_2 signal on the mass spectrometer indicated the liberation of chemically bound CO_2. The amount of released CO_2 was calculated by integration of the peak area and found to be 50% of the total uptake capacity of the MOF under these conditions. The regenerated IRMOF-74-III-CH_2NH_2 showed a breakthrough time as long as the one for the first run (Figure S19). This indicates that amine functionalities incorporated into the IRMOF-74-III require moderate regeneration conditions compared to MEA (ca. 120 °C) and other amine-functionalized MOFs.[7a] As a control experiment, we subjected IRMOF-74-III-CH_3 under the same conditions used for IRMOF-74-III-CH_2NH_2 and found a longer breakthrough time (1380 ± 10 s g^{-1});[12] however, upon purging the sample with nitrogen, all adsorbed CO_2 was recovered, indicating, as expected, no carbamate formation (Figure S20).

Both IRMOF-74-III-CH_2NH_2 and -CH_3 were examined by similar breakthrough experiments, but now in the presence of water. Prior to the breakthrough measurements, wet nitrogen with 65% RH was introduced to the adsorbent bed until the water concentration of the effluent showed a constant value (>16 h). To estimate the breakthrough time in the presence of water, we introduced a gas mixture containing 16% of dry CO_2

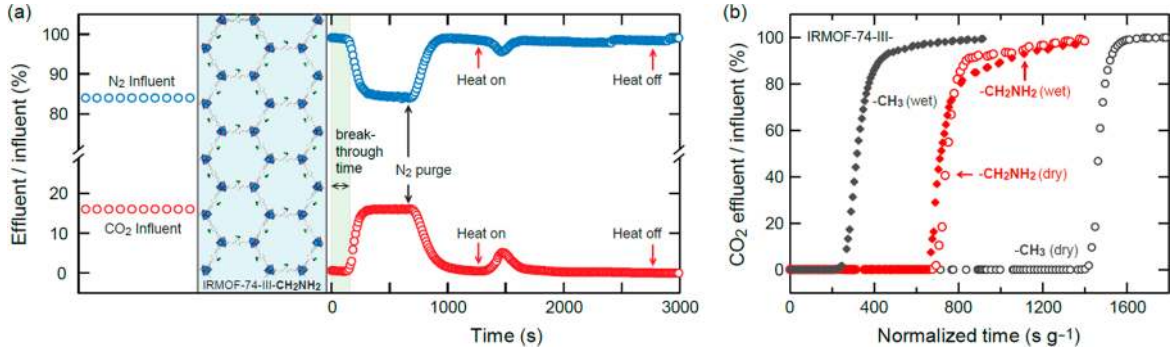

Figure 3. (a) IRMOF-74-III-CH_2NH_2 breakthrough cycle under dry conditions. Breakthrough time is highlighted in light blue. (b) Breakthrough curves for IRMOF-74-III-CH_3 under dry conditions (gray empty markers) and wet conditions (gray filled markers), and for IRMOF-74-III-CH_2NH_2 under dry conditions (red empty markers) and in the presence of water (red filled markers).

dx.doi.org/10.1021/ja503296c | J. Am. Chem. Soc. 2014, 136, 8863−8866

and 84% of wet nitrogen (65% RH). IRMOF-74-III-CH_2NH_2 showed a breakthrough time nearly identical to that observed under dry conditions (610 ± 10 s g^{-1}) (Figure 3b), while the breakthrough time of IRMOF-74-III-CH_3 under wet conditions showed an 80% decrease compared to that in the absence of moisture. This behavior indicates that the CO_2 uptake in IRMOF-74-III-CH_3 is, as expected, mainly attributable to the open magnesium sites, which are occupied by water molecules under humid conditions.[12] In IRMOF-74-III-CH_2NH_2, the CO_2 uptake takes place at the linker amine sites, while the open magnesium sites are not accessible under dry nor humid conditions (section S7, SI); therefore, the effect of water on the CO_2 uptake should be negligible. This is also supported by the dissimilar desorption behavior compared to IRMOF-74-III-CH_3 (Figures 3a and S20).

IRMOF-74-III-CH_2NH_2 with bound CO_2 was regenerated by purging with dry nitrogen followed by heating at 90 °C to remove the CO_2. A second cycle of humidification and CO_2 uptake was applied as explained above to obtain a nearly identical breakthrough time (600 ± 10 s g^{-1}) (section S9, SI). We further note that the PXRD pattern of the sample after these cycles was identical to that of the activated sample, thus indicating full preservation of IRMOF-74-III-CH_2NH_2 structure throughout the CO_2 capture process (Figure S16).

■ ASSOCIATED CONTENT

Supporting Information

Detailed organic linkers and MOFs synthetic procedures, including characterization by NMR spectra, PXRD, nitrogen adsorption, breakthrough experiments, and complete refs 4b, 5g, and 9. This material is available free of charge via the Internet at http://pubs.acs.org.

■ AUTHOR INFORMATION

Corresponding Author

yaghi@berkeley.edu

Notes

The authors declare no competing financial interest.

■ ACKNOWLEDGMENTS

This work was partially supported for synthesis and characterization by BASF SE (Ludwigshafen, Germany), gas adsorption by U.S. Department of Defense, Defense Threat Reduction Agency (HDTRA 1-12-1-0053), and carbon dioxide adsorption studies by the U.S. Department of Energy, Office of Science, Office of Basic Energy Sciences, Energy Frontier Research Center (DE-SC0001015).

■ REFERENCES

(1) Granite, E. J.; Pennline, H. W. *Ind. Eng. Chem. Res.* **2002**, *41*, 5470.

(2) (a) Li, G.; Xiao, P.; Webley, P.; Zhang, J.; Singh, R.; Marshall, M. *Adsorption* **2008**, *14*, 415. (b) Liu, J.; Thallapally, P. K.; McGrail, B. P.; Brown, D. R.; Liu, J. *Chem. Soc. Rev.* **2012**, *41*, 2308. (c) Yu, J.; Balbuena, P. B. *J. Phys. Chem. C* **2013**, *117*, 3383.

(3) (a) Sharma, S. D.; Azzi, M. *Fuel* **2014**, *121*, 178. (b) Gouedard, C.; Picq, D.; Launay, F.; Carrette, P.-L. *Int. J. Greenhouse Gas Control* **2012**, *10*, 244. (c) Johnson, J. *Chem. Eng. News* **2004**, *82* (51, Dec 21), 36.

(4) (a) Li, D.; Furukawa, H.; Deng, H.; Liu, C.; Yaghi, O. M.; Eisenberg, D. S. *Proc. Natl. Acad. Sci. U.S.A.* **2014**, *111*, 191. (b) Nugent, P.; et al. *Nature* **2013**, *495*, 80. (c) Hao, G.-P.; Li, W.-C.; Qian, D.; Wang, G.-H.; Zhang, W.-P.; Zhang, T.; Wang, A.-Q.; Schüth, F.; Bongard, H.-J.; Lu, A.-H. *J. Am. Chem. Soc.* **2011**, *133*, 11378.

(5) (a) Sumida, K.; Rogow, D. L.; Mason, J. A.; McDonald, T. M.; Bloch, E. D.; Herm, Z. R.; Bae, T.-H.; Long, J. R. *Chem. Rev.* **2012**, *112*, 724. (b) Gassensmith, J. J.; Furukawa, H.; Smaldone, R. A.; Forgan, R. S.; Botros, Y. Y.; Yaghi, O. M.; Stoddart, J. F. *J. Am. Chem. Soc.* **2011**, *133*, 15312. (c) Britt, D.; Furukawa, H.; Wang, B.; Glover, T. G.; Yaghi, O. M. *Proc. Natl. Acad. Sci. U.S.A.* **2009**, *106*, 20637. (d) Horike, S.; Kishida, K.; Watanabe, Y.; Inubushi, Y.; Umeyama, D.; Sugimoto, M.; Fukushima, T.; Inukai, M.; Kitagawa, S. *J. Am. Chem. Soc.* **2012**, *134*, 9852. (e) Xiang, S.; He, Y.; Zhang, Z.; Wu, H.; Zhou, W.; Krishna, R.; Chen, B. *Nat. Commun.* **2012**, *3*, 954. (f) Li, T.; Sullivan, J. E.; Rosi, N. L. *J. Am. Chem. Soc.* **2013**, *135*, 9984. (g) Li, B.; et al. *Angew. Chem., Int. Ed.* **2012**, *51*, 1412. (h) Wriedt, M.; Sculley, J. P.; Yakovenko, A. A.; Ma, Y.; Halder, G. J.; Balbuena, P. B.; Zhou, H.-C. *Angew. Chem., Int. Ed.* **2012**, *51*, 9804. (i) Deria, P.; Mondloch, J. E.; Tylianakis, E.; Ghosh, P.; Bury, W.; Snurr, R. Q.; Hupp, J. T.; Farha, O. K. *J. Am. Chem. Soc.* **2013**, *135*, 16801. (j) Lu, A.-H.; Hao, G.-P. *Annu. Rep. Prog. Chem., Sect. A: Inorg. Chem.* **2013**, *109*, 484. (k) Hedin, N.; Andersson, L.; Bergstrom, L.; Yan, J. *Appl. Energy* **2013**, *104*, 418. (l) Samanta, A.; Zhao, A.; Shimizu, G. K. H.; Sarkar, P.; Gupta, R. *Ind. Eng. Chem. Res.* **2012**, *51*, 1438.

(6) (a) Furukawa, H.; Cordova, K. E.; O'Keeffe, M.; Yaghi, O. M. *Science* **2013**, *341*, 974. (b) Furukawa, H.; Cordova, K. E.; O'Keeffe, M.; Yaghi, O. M. *Science* **2013**, *341*, 1230444.

(7) (a) McDonald, T. M.; Lee, W. R.; Mason, J. A.; Wiers, B. M.; Hong, C. S.; Long, J. R. *J. Am. Chem. Soc.* **2012**, *134*, 7056. (b) Planas, N.; Dzubak, A. L.; Poloni, R.; Lin, L.-C.; McManus, A.; McDonald, T. M.; Neaton, J. B.; Long, J. R.; Smit, B.; Gagliardi, L. *J. Am. Chem. Soc.* **2013**, *135*, 7402. (c) Lee, W. R.; Hwang, S. Y.; Ryu, D. W.; Lim, K. S.; Han, S. S.; Moon, D.; Choi, J.; Hong, C. S. *Energy Environ. Sci.* **2014**, *7*, 744. (d) Cao, Y.; Song, F.; Zhao, Y.; Zhong, Q. *J. Environ. Sci.* **2013**, *25*, 2081. (e) Demessence, A.; D'Alessandro, D. M.; Foo, M. L.; Long, J. R. *J. Am. Chem. Soc.* **2009**, *131*, 8784.

(8) (a) Lu, W.; Sculley, J. P.; Yuan, D.; Krishna, R.; Wei, Z.; Zhou, H.-C. *Angew. Chem., Int. Ed.* **2012**, *51*, 7480. (b) Arstad, B.; Fjellvåg, H.; Kongshaug, K. O.; Swang, O.; Blom, R. *Adsorption* **2008**, *14*, 755. (c) Qiao, Z.; Zhou, J.; Lu, X. *Fluid Phase Equilib.* **2014**, *362*, 342.

(9) Deng, H.; et al. *Science* **2012**, *336*, 1018.

(10) (a) Cohen, S. M. *Chem. Rev.* **2012**, *112*, 970. (b) Lun, D. J.; Waterhouse, G. I. N.; Telfer, S. G. *J. Am. Chem. Soc.* **2011**, *133*, 5806.

(11) Pinto, M. L.; Mafra, L.; Guil, J. M.; Pires, J.; Rocha, J. *Chem. Mater.* **2011**, *23*, 1387.

(12) Liu, J.; Benin, A. I.; Furtado, A. M. B.; Jakubczak, P.; Willis, R. R.; LeVan, M. D. *Langmuir* **2011**, *27*, 11451.